JMEPEG (2017) 26:4964–4969
DOI: 10.1007/s11665-017-2927-9

1059-9495/$19.00

Improved Functional Properties and Efficiencies of Nitinol Wires Under High-Performance Shape Memory Effect (HP-SME)

R. Casati, F. Saghafi, C.A. Biffi, M. Vedani, and A. Tuissi

(Submitted November 18, 2016; in revised form May 16, 2017; published online September 19, 2017)

Martensitic Ti-rich NiTi intermetallics are broadly used in various cyclic applications as actuators, which exploit the shape memory effect (SME). Recently, a new approach for exploiting austenitic Ni-rich NiTi shape memory alloys as actuators was proposed and named high-performance shape memory effect (HP-SME). HP-SME is based on thermal recovery of de-twinned martensite produced by mechanical loading of the parent phase. The aim of the manuscript consists in evaluating and comparing the fatigue and actuation properties of austenitic HP-SME wires and conventional martensitic SME wires. The effect of the thermomechanical cycling on the actuation response and the changes in the electrical resistivity of both shape memory materials were studied by performing the actuation tests at different stages of the fatigue life. Finally, the changes in the transition temperatures before and after cycling were also investigated by differential calorimetric tests.

Keywords functional properties, NiTi, shape memory wires, thermomechanical cycling

1. Introduction

NiTi is a widely used shape memory alloy (SMA) for commercial application in several industrial fields. NiTi restore great amounts of deformation either upon heating (shape memory effect) or unloading (pseudoelastic effect) through a phase transformation between a high-temperature cubic parent phase, termed austenite, and a low-temperature product phase, named martensite, by exploiting a shear-like mechanism called de-twinning (Ref 1, 2). Since the functional properties of the NiTi SMAs are strictly dependent on their chemical composition, variation of the Ni content of the material leads to thoroughly dissimilar behaviors of the material at environmental conditions (Ref 3).

Ti-rich SMAs, which are in martensitic phase at room temperature, show the so-called shape memory effect (SME). This group of SMAs is mostly used in micro-/linear actuators, optical image stabilizers and other fields of industry such as robotics, aerospace and automotive (Ref 4-8). The application of an external force to a martensitic SMA leads to the formation of de-twinned martensite, accompanied by high values of deformation (Ref 1, 2). The heating of misshaped SMA above a certain temperature austenite start (A_s) leads to the transformation of martensite into austenite and allows the macroscopic deformation to be recovered. The entire austenitic phase is settled when the temperature exceeds the austenite finish (A_f). In a cooling process, the pre-deformed self-accommodated martensite is regenerated. The temperatures in which the martensite starts to be created until the completion of the transformation are named martensite start (M_s) and martensite finish (M_f), respectively (Ref 1, 2). In Fig. 1(a), a schematic of the SME is depicted.

Ni-rich SMAs, mainly consisting of austenite at room temperature, show the pseudoelastic or superelastic (SE) behavior. The austenitic SMAs are widely exploited in biomedical field, ranging from vascular stents to medical devices, thanks to their excellent biocompatibility and corrosion resistance (Ref 9, 10). Furthermore, these types of smart materials are also used in damping applications (Ref 11). Austenitic SMAs enable re-establishment of high magnitudes of strain (up to 10%) without accumulation of plastic deformation. In this case, the driving force for the martensitic transformation is the applied stress. In particular, by exceeding the imposed stress from a critical extent (SE plateau), the stress-induced martensite (SIM) and accordingly the deformation are produced. Upon unloading, the imposed deformation is totally recovered. A schematic of SE effect is shown in Fig. 1(b).

We have recently proposed austenitic SMAs as suitable materials for actuators. They are able to recover high strain values under extremely high stress (up to 1 GPa). Austenitic SMAs achieve unique performance by a phenomenon that we called high-performance shape memory effect (HP-SME), which exploits the thermal cycling of the SIM (Ref 12). As an austenitic SMA (e.g., Ni-rich NiTi) is loaded up to a critical stress, SIM is produced. By heating the SIM above A_f under constant applied force, the material shifts back due to the stabilization of the austenite and the macroscopic deformation is recovered. By cooling the material down to the environmental temperature, a complete SIM state is reproduced and the deformation is restored. Figure 1(c) schematically shows the cyclic process of HP-SME. Therefore, the main difference between actuators based on SME and actuators based on HP-

R. Casati, F. Saghafi, and **M. Vedani**, Department of Mechanical Engineering, Politecnico di Milano, Via La Masa 1, Milan, Italy; and **C.A. Biffi** and **A. Tuissi**, National Research Council, Institute of Condensed Matter Chemistry and Technologies for Energy, CNR-ICMATE, Corso Promessi Sposi 29, Lecco, Italy. Contact e-mail: riccardo.casati@polimi.it.

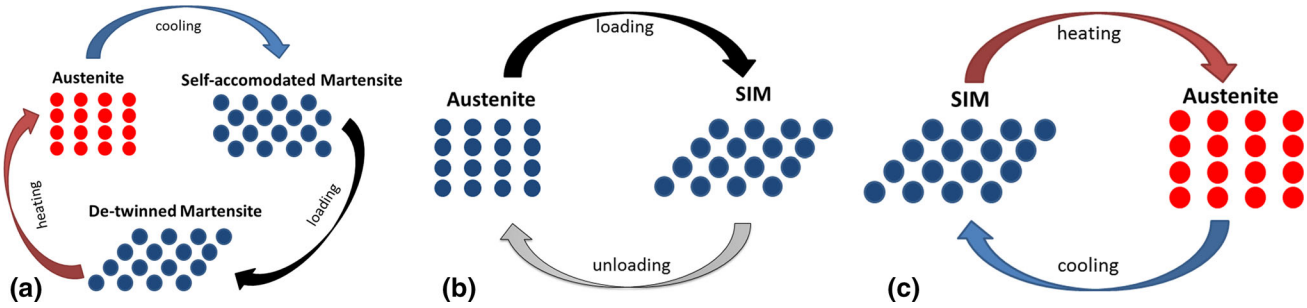

Fig. 1 Schematic view of the (a) shape memory effect (SME), (b) superelastic effect (SE), (c) high-performance shape memory effect (HP-SME)

SME is that the former rely on thermal cycling of de-twinned martensite, whereas the latter rely on thermal cycling of SIM. SME is almost unaffected by the operative temperature, whereas critical stress for stress-induced martensite is affected by the temperature, according to the Clausius–Clapeyron equation. This could be a limit when the operating temperature varies in a wide range. Further details about HP-SME are given in Ref 12 and 13.

In our previous work (Ref 12), we compared Ti-rich SME and Ni-rich HP-SME thin wires under constant stress (250 and 800 MPa, respectively), and we first showed that a much higher actuating force can be produced by exploiting the HP-SME within the same temperature range [20-160 °C]. The aim of this work consists instead in evaluating and comparing the properties of HP-SME and SME NiTi wires during fatigue life. The effect of cycling on the actuation response, the electrical resistivity and the transformation temperatures of SME and HP-SME specimens is hereafter presented.

2. Materials and Methods

2.1 Materials

Two types of commercial shape memory wires, i.e., SME martensitic ($Ni_{49}Ti_{51}$ at.%) and HP-SME austenitic ($Ni_{51}Ti_{49}$ at.%) wires, with nominal diameter of 300 μm were provided by SAES Getters Spa. Characteristic transformation temperature has been characterized by differential scanning calorimetry analysis. The thermograms are shown in section 3. They were divided into pieces of almost 100 mm in length, and they were used as specimens in the fatigue and actuation tests. The wires were coated with Ti oxide.

2.2 Fatigue and Actuation Tests

The fatigue and actuation tests were performed on the SMA wires by the use of an experimental apparatus, designed and constructed for this purpose. Figure 2 schematically depicts the configuration of components in the experimental rig. Each wire was vertically placed in a rig made up of aluminum profiles. The wires were positioned between an upper clamp fixed to the structure and a lower one connected to a load bar. The weights were mounted on a circular thin plate screwed at the end of the load bar in order to impose an axial constant stress to the wires. The aluminum rig was insulated from the upper clamp by means of a plastic plate. An electrical step-form current pulse, supplied by a programmable Aim-TTiCPX 400SP DC power

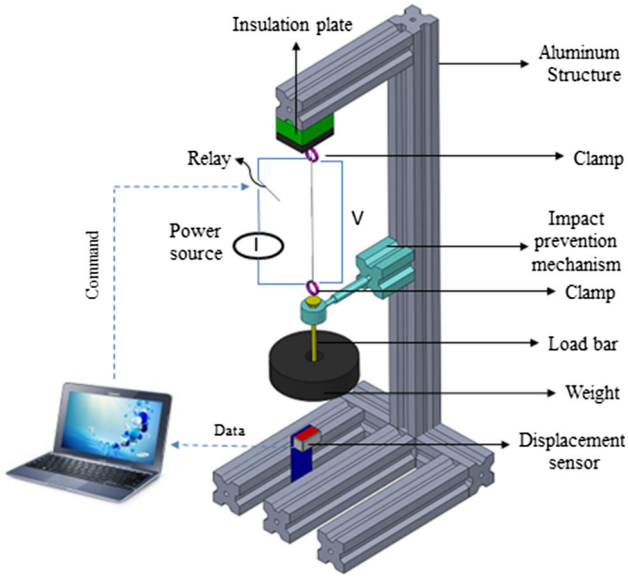

Fig. 2 Schematic configuration of the experimental rig

source, was used to heat up the wires by Joule effect. A short-range proximity distance sensor with analog voltage output (SICK, OD1-B035H15U14) was used to record the instantaneous position of the wires. A National Instrument data acquisition device (NI-DAQ), equipped by an analog input (NI-9215) to acquire data from the sensor and a relay (NI-9481) to pass/stop the current, was used. The tests were controlled by NI LabVIEW programs, and the operating parameters such as the displacement of the wires and the cooling time were set by the operator.

SME and HP-SME specimens were axially stressed at 200 and 600 MPa, respectively. The two stress levels were chosen in order to induce SIM in the Ni-rich wire and to de-twin martensite in the Ti-rich wire. At this purpose, the tensile curves of the two wires are shown in Fig. 3.

Then, they were heated by a step current pulse of 1A under strain control. The cooling process of the wire specimens was performed by switching off the current for 10 s, as soon as a fixed recovered displacement was achieved. The recovered displacement was set in order to achieve a corresponding strain of 2.3%. The temperature of the wire, which is function of time and intensity of the current pulse (Joule effect), was not measured, but by interrupting the strain at a fixed value, the overheating of the material was avoided. The NI LabVIEW program recorded the lengths of the wires after heating/cooling

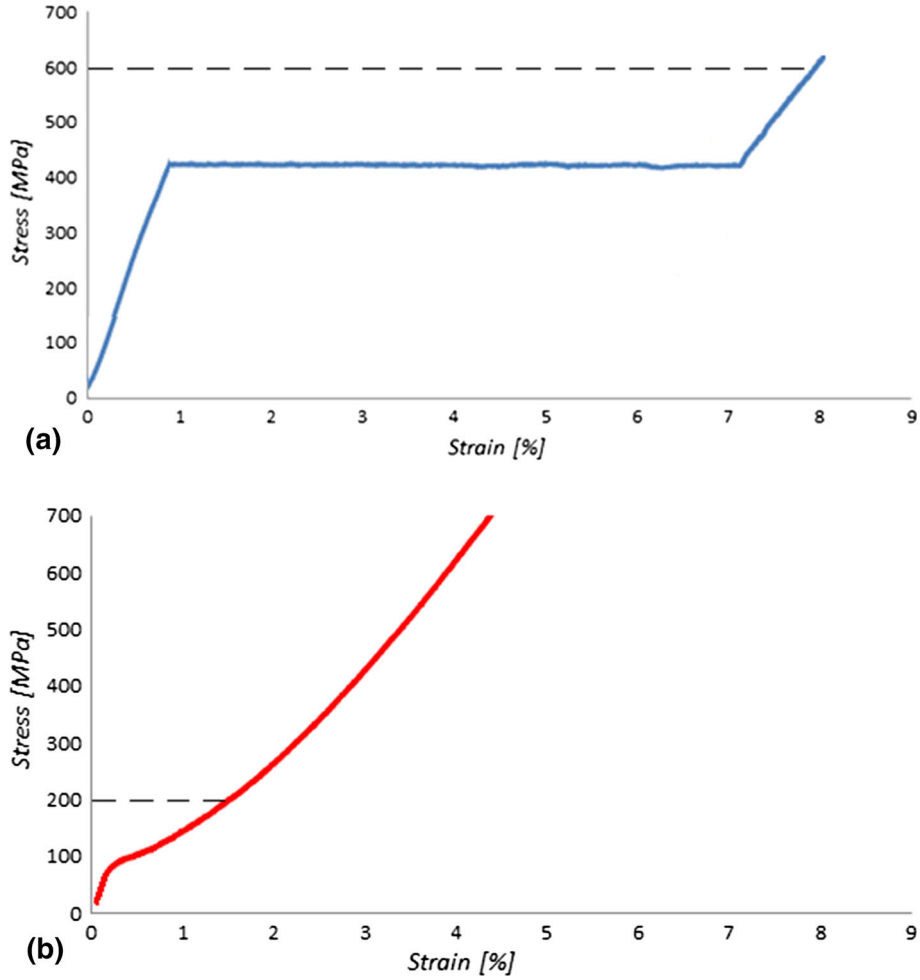

Fig. 3 Tensile curve of (a) the SME (Ti-rich) wire and of (b) the HP-SME (Ni-rich) wire

cycles, and accordingly the strain was computed after each thermomechanical loop. The functional fatigue tests (thermomechanical cycling, TMC) were performed for 7500 cycles. During the fatigue tests, the actuation response of the SME and HP-SME wires at the 1st, 100th, 1000th and 7500th cycles was investigated.

It is worth noting that 200 MPa was used for martensitic wire, which is a typical applied stress in actuators based on SME, and 600 MPa was used for austenitic wires, so as to induce a fully SIM structure.

2.3 Resistivity Tests and Efficiency

The potential difference was measured with a voltmeter connected at the two wire clamps. Thus, the resistance was measured by 4-point probes method. The electrical resistivity (ρ) change of the SMA wires is evaluated during actuation tests as stated hereunder:

$$\rho = \frac{V\pi d^2}{4LI} \quad \text{(Eq 1)}$$

where V is the voltage, I is the current density, d and L are the actual diameter and length of the wire. The wire diameter was calculated, assuming that the phase transformation occurs at constant volume.

The actuator efficiency, η, is calculated as follows:

$$\eta = \frac{\text{Output Work}}{\text{Input Energy}} \times 100 = \frac{F\Delta l}{\int_{t=0}^{t=t_f} VI\mathrm{d}t} \times 100 \quad \text{(Eq 2)}$$

where F is the applied load, Δl is the recovered displacement, t is the time and t_f is the actuation time.

2.4 Differential Scanning Calorimetry (DSC) Tests

DSC tests were carried out before and after TMC. A TA INSTRUMENT Q100 with a scanning rate of 10 °C/min over a temperature range from 123 to 423 K was utilized to determine the transformation temperatures.

3. Results and Discussion

In Fig. 4, the trends of the maximum and minimum strains of both types of wires are plotted as a function of number of cycles. The maximum and minimum strain values were detected after the heating and cooling steps, respectively. During cycling, the wires plastically deform and become longer. Thermomechanical cycling leads to microstructural modifications such as a rise in dislocations density (Ref 1, 2). The recovered strain decreased by increasing the number of cycles for both samples. The HP-SME and the SME specimens

stored 0.03 and 0.1% of unrecoverable deformation after 7500 cycles, respectively. Even though the HP-SME wire was subjected to higher stress (600 MPa), it shows a slightly higher cycling stability. The graph in Fig. 4 shows that the two wires have similar functional cyclic behaviors and points out the main advantage of HP-SME: The austenitic wire is able to produce higher work (three times in this case) with respect to martensitic wire for thousands of cycles.

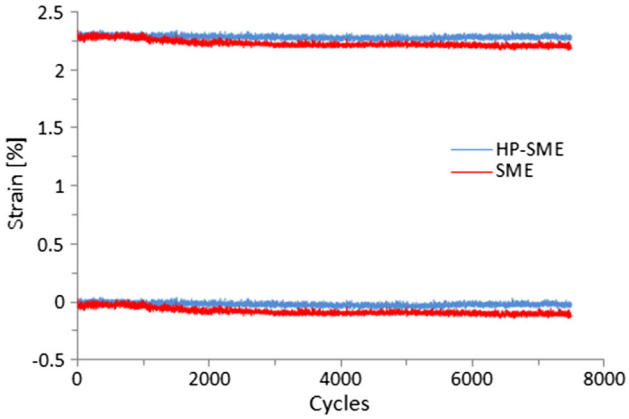

Fig. 4 Maximum and minimum recovered strain of HP-SME (under 600 MPa) and SME (under 200 MPa) wires vs. number of cycles

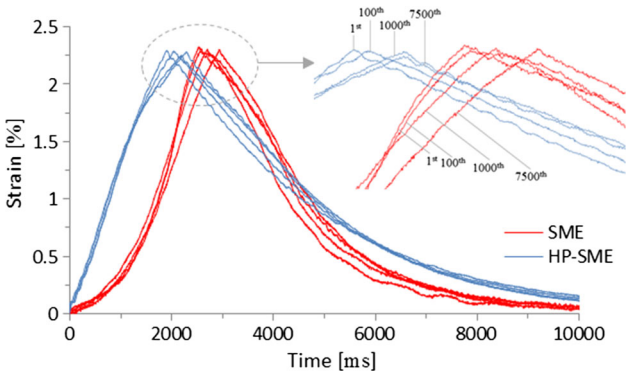

Fig. 5 Actuation behavior of HP-SME and SME wires at different stages of the TMC

Figure 5 shows the actuation response of HP-SME and SME wires at different stages of the TMC. The time required for the SME wire to recover the strain of 2.3% at the first cycle was 2513 ms, while this value was extended by 53, 135 and 271 ms after 100, 1000 and 7500 cycles, respectively. This implies that the actuation time of the SME wire is expanded by 14.7% after 7500 cycles. On the other hand, the HP-SME wire retrieved the same amount of strain in an almost linear path by 1970 ms on its first cycle. In the same manner, the actuation response of the HP-SME wire was prolonged by 31, 203 and 262 ms after the same thermomechanical loops, and as a consequence, the time taken by the HP-SME wire to recover the strain of 2.3% was increased by 13.2% after TMC. Therefore, it is possible to assert that the rise in the actuation time of the HP-SME wire under the constant stress of 600 MPa is slightly lower than the SME one under 200 MPa, after 7500 cycles. Considering the slope of the graphs, the HP-SME wire showed a faster quasi-linear response upon heating and a slower curved one during the cooling with respect to the SME wire. The linearity of the heating curve for the HP-SME wire was especially considerable at the 1st and 100th cycles, and it was reduced by increasing the number of cycles. On the contrary, the SME wire was instead faster upon cooling, especially by proceeding with the TMC. The cooling curves show different behaviors for the two wires, which can be ascribed to several phenomena, namely maximum reached temperature (according to the Clausius–Clapeyron equation (Ref 14), thermal diffusivity of the material and phase transformation, as it was extensively described in previous works (Ref 15, 16).

The DSC thermograms of the wires before and after TMC are depicted in Fig. 6, and the main characteristic temperatures are summarized in Table 1. The calorimetry test allowed to state that the SME and HP-SME wires were, respectively, in martensitic and austenitic phases at room temperature. In both cases, before TMC, a two-stage direct transformation was observed during the cooling (B2 → R → B19′) (Ref 1, 2).

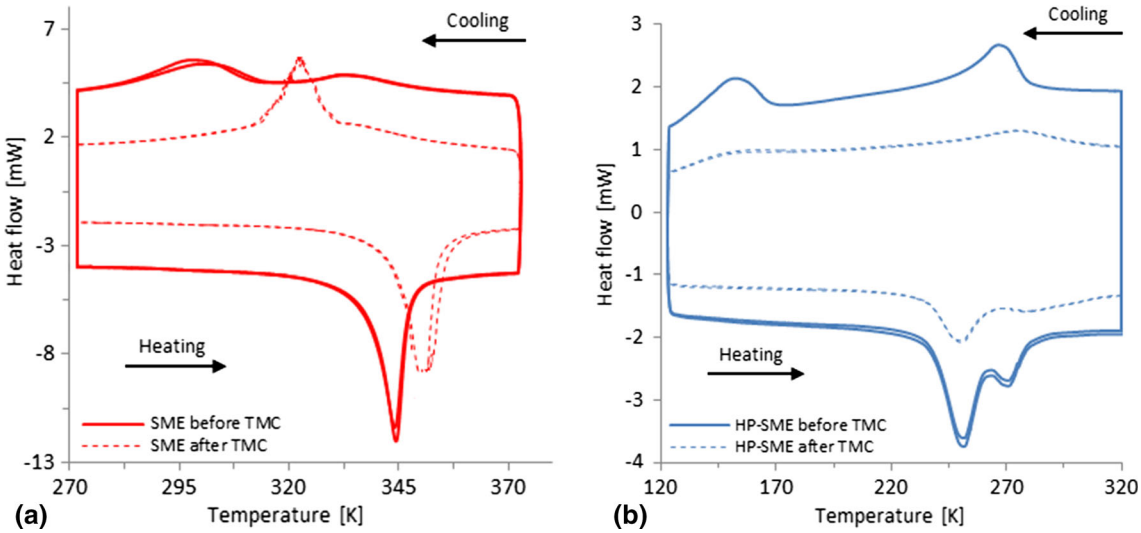

Fig. 6 DSC thermograms before and after TMC of the (a) SME wire and (b) HP-SME wire

Table 1 Characteristic temperatures derived from DSC

	Cooling				Heating			
	R_s, °C	R_f, °C	M_s, °C	M_f, °C	R_s, °C	R_f, °C	A_s, °C	A_f, °C
SME before cycling	73.3	52.2	38.9	3.6	…	…	61.2	73.7
SME after cycling	…	…	58.4	38.3	…	…	66.8	83.8
HP-SME before cycling	14.3	−21.3	−99.8	< −150	−42.0	−12.9	−12.9	13.5
HP-SME after cycling	35.3	−34.3	−89.1	< −150	−39.9	−5.3	−5.3	44.2

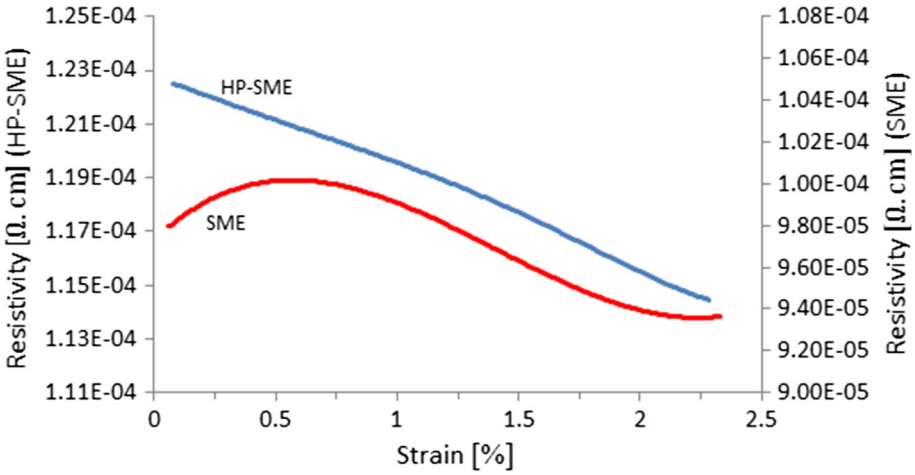

Fig. 7 Comparison between ER change of SME and HP-SME wires during the heating process

Upon heating, a single-stage inverse transformation (B19′ → B2) for the SME wire and a double-stage inverse transformation (B19′ → R → B2) for the HP-SME one occurred before TMC (Ref 1, 2). After cycling, the phase transformation temperatures shifted toward the higher temperatures and the peaks became smoother. The increase in the transition temperatures is responsible of the extension in actuation time.

Figure 7 illustrates the comparison between the electrical resistivity changes of the SMA wires versus strain, upon the heating process. The resistivity is an intrinsic temperature-dependent property of each material, which is not affected by shape changes. Previous researches have shown that the austenite exhibits lower resistivity compared to martensitic phase (Ref 17, 18). The two wires show different behaviors, i.e., the electrical resistivity of the SME wire first increased from 9.80E−05 to 1.00E−04 Ωcm and then almost linearly decreased to 9.35E−05 Ωcm. In SME wire, the R phase, which is usually characterized by an higher resistivity, may play a fundamental role in increasing resistivity values of SME for strain values < 1% (Ref 19). On the other hand, the resistivity of the HP-SME wire continuously decreased from 1.23E−04 to 1.15E−04 Ωcm in an almost linear manner. There is no evidence of R phase effect in the HP-SME actuating curve. The total amount of resistivity change for both wires was the same and almost equal to 6%. Since, the ρ–ε curve of the HP-SME wire was much more linear with respect to the SME one, HP-SME wires can be preferably employed as a high-accuracy sensing elements in position controlling of the actuator systems. No significant resistivity variation was registered before and after TMC in both the wires.

The efficiency of the two actuators is evaluated according to Eq 2. The η of the HP-SME-based actuator revealed to be 7.1%, while that of the SME-based actuator was 0.9%. This result is extremely interesting for all those applications in which SMA active elements are supplied by batteries. Energy savings might be a key point to introduce SMAs in this industrial sector.

4. Conclusion

The thermomechanical fatigue and actuation tests of commercial NiTi wires (300 μm) subjected to HP-SME (by applying 600 MPa) and SME (by applying 200 MPa) were experimented, and the main outcomes are summarized below.

- The fatigue tests showed that, despite the similar TMC behavior of the two commercial NiTi wires, after 7500 cycles, the HP-SME (under 600 MPa) shows a slight better stability with an accumulated unrecoverable deformation of 0.03% with respect to 0.1% of traditional SME wire loaded at lower stress (200 MPa).
- The actuation tests showed a faster and linear actuating strain/time behavior for HP-SME wire. At first cycle, actuating times of 1970 and 2513 ms were detected for HP-SME and SME wires, respectively. By increasing the number of cycles, the time required by both the SMA wires to reach a constant-controlled strain of 2.3% increased. However, the actuation time of the SME wire was slightly greater than that of the HP-SME one after 7500 cycles; thus, the latter show a more stable actuating response.
- Comparison between the changes in electrical resistivity

of the SMA wires highlighted that the ρ–ε curve of the HP-SME wire features a very promising linear behavior that can be useful for positioning control in actuation devices.
- Thanks to HP-SME, the austenitic wires, industrially employed for developing superelastic devices mainly for biomedical applications, can now be used for developing a new class of shape memory actuators with increased performances in terms of recoverable forces (up to four times), linear resistance/strain behavior, faster actuating times and energy efficiency.

Acknowledgments

The authors gratefully thank SAES Getters Spa for material supply.

References

1. K. Otsuka and C.A. Wayman, *Shape Memory Materials*, Cambridge University Press, Cambridge, 1998
2. K. Otsuka and X. Ren, Physical Metallurgy of Ti–Ni-Based Shape Memory Alloys, *Prog. Mater Sci.*, 2005, **50**, p 511–678
3. J. Frenzel, E.P. George, A. Dlouhy, C.H. Somsen, M.F.X. Wagner, and G. Eggeler, Influence of Ni on Martensitic Phase Transformations in NiTi Shape Memory Alloys, *Acta Mater.*, 2010, **58**, p 3444–3458
4. J.M. Jani, M. Leary, A. Subic, and M.A. Gibson, A Review of Shape Memory Alloy Research, Applications and Opportunities, *Mater. Des.*, 2014, **56**, p 1078–1113
5. M. Kohl and K.D. Skrobanek, Linear Microactuators Based on the Shape Memory Effect, *Sens. Actuators A*, 1998, **70**, p 104–111
6. M. Kohl, K.D. Skrobanek, E. Quandt, P. Schlossmacher, A. Schussler, and D.M. Allen, Development of Microactuators Based on the Shape Memory Effect, *Journal de physique*, 1995, **IV**(C8), p 1187–1192
7. M. Kohl, *Shape Memory Actuators*, Springer, Berlin, 2004
8. J. Van Humbeeck, Non-medical Applications of Shape Memory Alloys, *Mater. Sci. Eng. A*, 1999, **273–275**, p 134–148
9. T. Duerig, A. Pelton, and D. Stoeckel, An Overview of Nitinol Medical Applications, *Mater. Sci. Eng. A*, 1999, **273–275**, p 149–160
10. S. Witold, M. Annick, H. Shunichi, Y. L'Hocine, and R. Jean, Medical Applications of Shape Memory Polymers, *Biomed. Mater.*, 2007, **2**, p S23
11. A. Tuissi, P. Bassani, R. Casati, M. Bocciolone, A. Collina, M. Carnevale, A. Lo Conte, and B. Previtali, Application of SMA Composites in the Collectors of the Railway Pantograph for the Italian High-Speed Train, *J. Mater. Eng. Perform.*, 2009, **18**, p 612–619
12. R. Casati, M. Vedani, and A. Tuissi, Thermal Cycling of Stress-Induced Martensite for High-Performance Shape Memory Effect, *Scr. Mater.*, 2014, **80**, p 13–16
13. R. Casati, C.A. Biffi, M. Vedani, and A. Tuissi, High Performance Shape Memory Effect in Nitinol Wire for Actuators with Increased Operating Temperature Range, *Funct. Mater. Lett.*, 2014, **7**, p 1450063
14. P. Wallants, M. De Binte, and J.R. Roos, *Z. Matalkl.*, 1979, **70**, p 113
15. C. Zanotti, P. Giuliani, G. Riva, and A. Tuissi, A ''Thermal Diffusivity of Ni–Ti SMAs'', *J. Alloys Compd.*, 2009, **473**, p 231–237
16. C. Zanotti, P. Giuliani, S. Arnaboldi, and A. Tuissi, Analysis of Wire Position and Operating Conditions on Functioning of NiTi Wires for Shape Memory Actuators, *JMEPEG*, 2011, **20**, p 688–696
17. H. Song, E. Kubica, and R. Gorbet, Resistance modelling of SMA wire actuators, in *International Workshop of Smart Materials, Structures & NDT in Aerospace Conference NDT in Canada 2011*
18. R. Featherstone and Y.H. Teh, Improving the Speed of Shape Memory Alloy Actuators by Faster Electrical Heating, in *ISER 2004*
19. V. Antonucci, G. Faiella, M. Giordano, F. Mennella, and L. Nicolais, Electrical Resistivity Study and Characterization During NiTi Phase Transformations, *Thermochim. Acta*, 2007, **462**, p 64–69